

A DETAILED MONTE CARLO INVESTIGATION OF THE TRICRITICAL REGION OF A BIAxIAL LIQUID CRYSTAL SYSTEM

CESARE CHICCOLI*, PAOLO PASINI†, and FRANCO SEMERIA‡

*Instituto Nazionale di Fisica Nucleare, Sezione di Bologna, Via Irnerio 46
40126 Bologna, Italy*

*E-mail: chiccoli@bo.infn.it

†E-mail: pasini@bo.infn.it

‡E-mail: semeria@bo.infn.it

CLAUDIO ZANNONI

*Dipartimento di Chimica Fisica ed Inorganica dell' Università
Viale Risorgimento 4, 40136 Bologna, Italy
E-mail: vz3bod7a@sirio.cineca.it*

Received 22 July 1998

Revised 1 October 1998

We study a lattice system of biaxial particles interacting with a second-rank anisotropic potential. We have performed detailed Monte Carlo calculations in the vicinity of the prolate-oblate dual value of molecular biaxiality. Our results confirm the second-order character of the transition in this limiting case.

Keywords: Computer Simulations; Liquid Crystals; Biaxial Nematics.

1. Introduction

Nematogen molecules are not uniaxial and could form, at least when the molecular biaxiality is large, a biaxial nematic phase where both the long and short axes present long range order. As a matter of fact this biaxial phase has been predicted to exist from Mean Field Theory (MFT)^{1,2} and from lattice^{3,4} and off-lattice⁵ computer simulations. Quite recently we have not only confirmed this existence but also determined the phase diagram and the full set of second-rank order parameters for a biaxial lattice model.⁴ In surprising contrast with theory, experiments have not yet shown, beyond any reasonable doubt, the existence of thermotropic biaxial nematic phases. Indeed the various claims put forward were based on optical observations and have recently been challenged by Deuterium NMR experiments,⁶ which are more straightforward to interpret.

The evidence now seems to show that large biaxialities λ , approaching the theoretical limit $\lambda_c = 1/\sqrt{6}$, which corresponds to the switching point from a distorted

prolate to a distorted oblate ellipsoid, are required for the observation of a biaxial nematic. This is probably because the biaxial nematic phase, occurring at a lower transition temperature than the uniaxial nematic one, competes with the more ordered, smectic or crystalline phases and, given that the temperature range of existence of typical nematics is about 10% from the transition,⁷ it follows that the observation is problematic except for the largest λ . How close the molecular biaxiality is to λ_c will depend on the detailed form of the (T_{NI}, λ) phase diagram in this region. In practice, the shape of the biaxial region in the phase diagram is reminiscent of a cusp with the biaxial nematic region becoming narrower near λ_c . It then becomes interesting to concentrate theoretical and simulation work in the region close to λ_c of the phase diagram, and this is what we plan to do here. In particular we concentrate on the dual point (also called bicritical Landau point) and its immediate neighborhood to examine in detail (i) the character of the biaxial to isotropic transition and (ii) the width of the biaxial cusp region. Our tools will be extensive Monte Carlo simulations as described in the next section.

2. The Model

Here we are concerned with the simplest rotationally invariant interaction between a pair of biaxial molecules^{3,4}

$$U(\omega_{ij}) = -\epsilon_{ij} \{ P_2(\cos \beta_{ij}) + 2\lambda [R_{02}^2(\omega_{ij}) + R_{20}^2(\omega_{ij})] + 4\lambda^2 R_{22}^2(\omega_{ij}) \} \quad (1)$$

We assume the particle positions to be fixed at the sites of a simple three-dimensional cubic lattice with L particles on the edge, containing therefore a total of $N = L^3$ sites. The strength of the interaction is given by ϵ_{ij} , taken to be a positive constant, ϵ , when particles i and j are nearest neighbors and zero otherwise. $\omega \equiv (\alpha, \beta, \gamma)$ is the set of Euler angles (we use Rose convention⁸) specifying the orientation of a molecule. The potential depends on the relative orientation ω_{ij} of the molecular pair, P_2 is a second Legendre polynomial and R_{mn}^L are combinations of Wigner functions symmetry — adapted for the D_{2h} group of the two particles. In particular the explicit expressions for the first few relevant terms are

$$P_2 = \frac{3}{2} \cos^2 \beta - \frac{1}{2} \quad (2)$$

$$R_{20}^2 = \frac{1}{2} \sqrt{\frac{3}{2}} \sin^2 \beta \cos 2\alpha \quad (3)$$

$$R_{02}^2 = \frac{1}{2} \sqrt{\frac{3}{2}} \sin^2 \beta \cos 2\gamma \quad (4)$$

$$R_{22}^2 = \frac{1}{4} (\cos^2 \beta + 1) \cos 2\alpha \cos 2\gamma - \frac{1}{2} \cos \beta \sin 2\alpha \quad (5)$$

λ is the parameter that accounts for the deviation from cylindrical molecular symmetry: when λ is zero, the potential in Eq. (1) reduces to the well-known Maier-Saupe or Lebwohl-Lasher⁹ P_2 potentials, while for nonzero λ the particles tend to

align not only their major axes, but also their faces. The same model has been studied on a fcc lattice by Luckhurst and Romano³ for $\lambda = 0.2$.

The biaxial potential in Cartesian form becomes

$$U = -\epsilon \left(\frac{3}{2} V_{33} - \lambda \sqrt{6} (V_{11} - V_{22}) + \lambda^2 (V_{11} + V_{22} - V_{12} - V_{21}) - \frac{1}{2} \right) \quad (6)$$

where $V_{ab} = (\mathbf{u}_a \cdot \mathbf{v}_b)^2$ and $\mathbf{u}_a, \mathbf{v}_b, a = 1, 2, 3$ are the three axes of the two interacting molecules. The parameters ϵ and λ will depend on molecular properties. In the special case of dispersive interactions, both parameters can be expressed in terms of the diagonal elements of the polarizability tensor α of the molecule. In this case

$$\lambda = \sqrt{\frac{3}{2}} \frac{\alpha_{xx} - \alpha_{yy}}{2\alpha_{zz} - (\alpha_{xx} + \alpha_{yy})} \quad (7)$$

$$\epsilon = (2\alpha_{zz} - (\alpha_{xx} + \alpha_{yy}))^2. \quad (8)$$

As can be seen after a little algebra, the potential is invariant by simultaneously changing the y and z axes of the molecules and substituting ϵ, λ with ϵ', λ'

$$\epsilon' = \epsilon \left(\frac{1 + \lambda\sqrt{6}}{2} \right)^2 \quad (9)$$

and

$$\lambda' = \frac{1}{\sqrt{6}} \left(\frac{4}{1 + \lambda\sqrt{6}} - 1 \right) \quad (10)$$

In the dispersion case this would correspond to exchanging α_{yy} and α_{zz} . The condition $\lambda' = \lambda$ corresponds to $\lambda = 1/\sqrt{6}$ and is the so-called self-dual case.² This means that for $\lambda > 1/\sqrt{6}$, that is for discotic molecules, one can change the y and z axes of the molecules and use the potential with the corresponding $\lambda' < 1/\sqrt{6}$ and ϵ' . In other words for $\lambda > 1/\sqrt{6}$ there is a mapping of the system to another system with $\lambda < 1/\sqrt{6}$ and the same potential, and all the thermodynamic results should be the same (of course the temperature $T = kT/\epsilon$ will correspond to $T' = kT/\epsilon'$).

3. Simulation Results

We have performed a set of independent simulations in the vicinity of the prolate-oblate dual value of the molecular biaxiality λ . In particular, different system sizes, ranging from 512 up to 64 000 particles, have been studied. A standard Metropolis algorithm¹⁰ with Periodic Boundary Conditions has been employed to update the lattice.

Several thermodynamic observables are calculated: energy, heat capacity and the full set of second-rank order parameters.⁴ The lowest temperature simulation is started from a completely aligned system; the following runs are produced in cascade starting from an equilibrated configuration of the nearest lower temperature. At least 60 000 equilibration Monte Carlo cycles (a cycle is a set of N attempted

moves) have been discarded at each temperature. The averages have been calculated on production runs of at least 40 000 cycles with runs of up to 200 000 cycles for selected temperatures. As we have shown in Ref. 4 it is preferable to perform simulations for $\lambda > 1/\sqrt{6} \approx 0.40825$ and then map the results onto a rescaled value of λ in the region $[0, 1/\sqrt{6}]$. This is convenient because the uniaxial — isotropic line in the transition temperature versus molecular biaxiality phase diagram appears rather flat below the prolate-oblate dual value of λ while the curve shows a rapid increase above this limiting molecular biaxiality. Then in the range $\lambda > 1/\sqrt{6}$ even a small variation of this parameter can produce a significant shift in the transition temperature. Thus we have chosen to perform larger simulations on a $40 \times 40 \times 40$ system for $\lambda = 0.40825, 0.420, 0.45, 0.5$.

In Fig. 1 we show curves for C_V^* at $\lambda = 1/\sqrt{6}, 0.420, 0.5$ as obtained from the larger system simulations ($N = 64\,000$). For $\lambda = 1/\sqrt{6}$ the results of C_V are superimposable moving from a system with 1000 particles⁴ to one with 64 000 molecules. This is profoundly different from what is found for a first order (even a weak first-order) transition like that of a three-dimensional Lebwohl-Lasher^{11,12} and confirms that the orientational phase transition at $\lambda = 1/\sqrt{6}$ has a second-order character. It can also be noticed that a small deviation (about 3%) in the molecular biaxiality is sufficient to detect the second transition from a biaxial phase to the nematic one. The temperature of this transition is shifted approximately 30% with

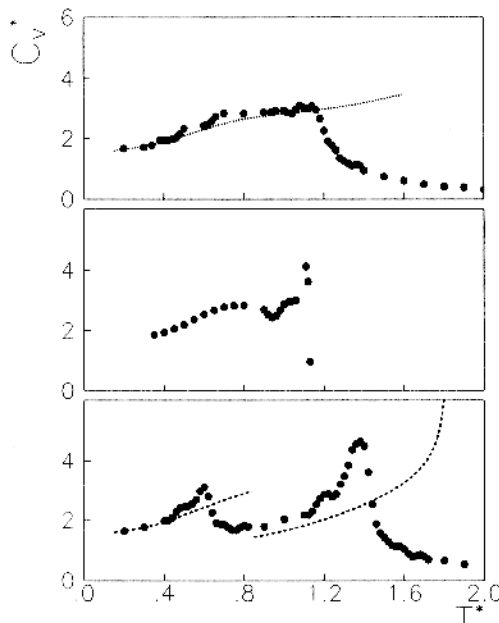


Fig. 1. Heat capacity, C_V^* , versus scaled temperature T^* as obtained from the simulations. Results for $\lambda = 0.40825$ (top), $\lambda = 0.420$ (middle), $\lambda = 0.500$ (bottom) on a 64,000 spin system are reported. The dotted lines represent the mean field predictions.

respect to the nematic–isotropic one for $\lambda = 0.420$. Then these simulations confirm that the peak of the cusp denoting the biaxial region in the phase diagram, reported in Fig. 2, is located at a lower temperature compared to the Mean Field Theory prediction. Moreover the uniaxial–biaxial curves forming the cusp increase very rapidly near λ_c and this confirms the difficulty in finding experimental evidence of the biaxial phase when using molecules with a molecular biaxiality not extremely close to the self-dual value. The bottom plate in Fig. 2 shows in detail the phase diagram of the transition temperatures versus the molecular biaxiality λ in the vicinity of the dual value where the limited amplitude of the biaxial nematic is apparent.

The phase transition at the dual point was predicted to be second-order using Mean Field Theory (MFT).^{1,2} However, this is of little value in itself given the known limitations of MF Theory, which neglects pair correlations, in studying phase transitions. On the other hand, our previous MC study had too few points and too small a sample to assess this characteristic.

Here we have also looked at the order parameters, shown in Figs. 3–6 calculated for $N = 1000$ and $N = 64\,000$ lattices, for a value of molecular biaxiality $\lambda = 0.40825$. The calculations have been performed using the procedure that we have

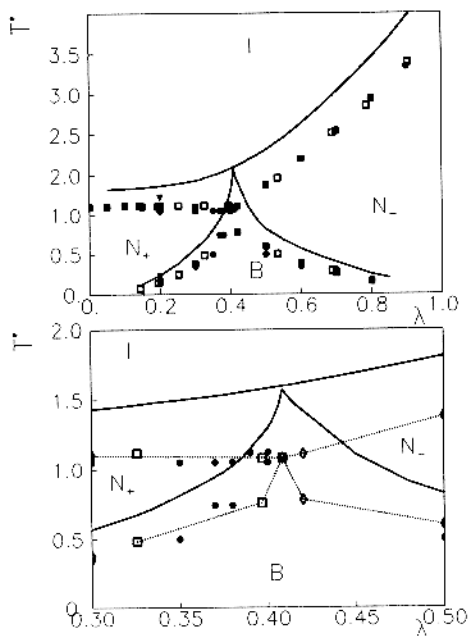


Fig. 2. The biaxial model phase diagram showing the reduced transition temperatures versus molecular biaxiality λ (top) and a close up in the vicinity of the limiting prolate–oblate value (bottom). MC results are shown as diamonds ($40 \times 40 \times 40$), full squares ($10 \times 10 \times 10$) and circles ($8 \times 8 \times 8$). Empty squares are points mapped from (λ, T^*) onto $(\lambda', T^{*'})$ (see text). The triangles at $\lambda = 0.2$ are from Ref. 3. MFT results are shown as continuous lines, while dotted lines are just a guide for the eye.

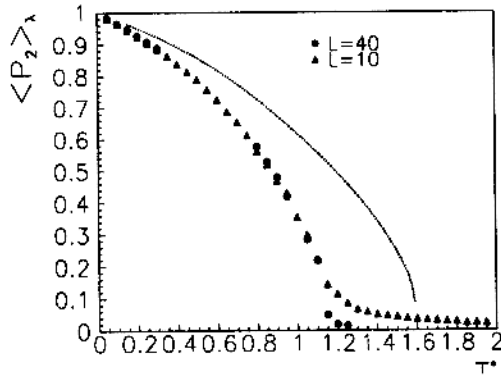


Fig. 3. The second-rank nematic order parameter $\langle P_2 \rangle$ as obtained from MC simulations on two lattice sizes.

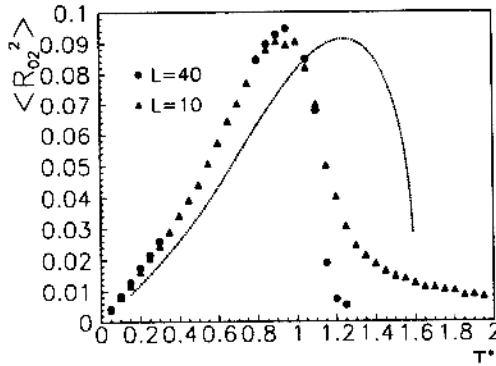


Fig. 4. The second-rank order parameter $\langle R_{02}^2 \rangle$ as obtained from MC simulations on two lattice sizes.

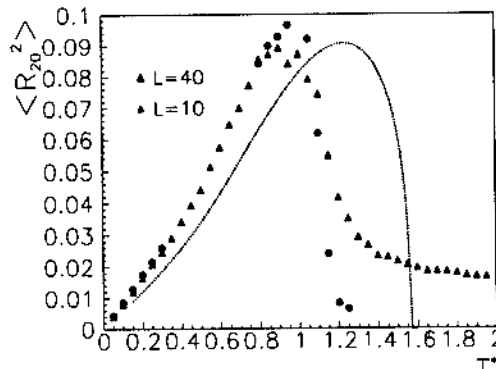


Fig. 5. The second-rank order parameter $\langle R_{20}^2 \rangle$ as obtained from MC simulations on two lattice sizes.

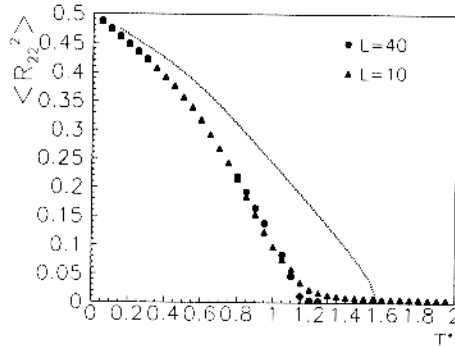


Fig. 6. The second-rank order parameter $\langle R_{22}^2 \rangle$ as obtained from MC simulations on two lattice sizes.

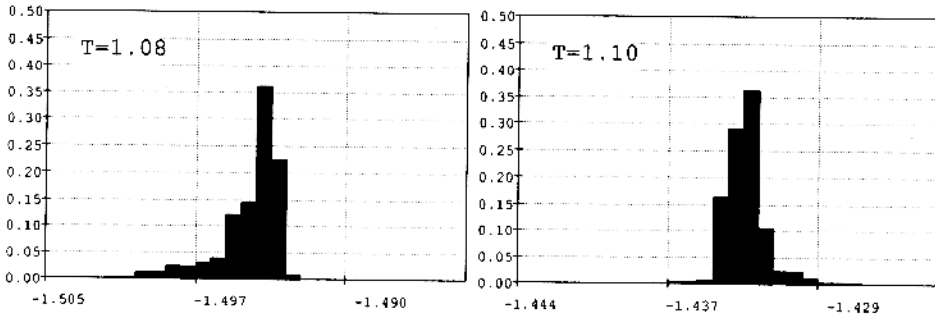


Fig. 7. The histogram of the energy per particle $\langle U^* \rangle$ as obtained over 100 000 MC cycles on a $40 \times 40 \times 40$ lattice at two selected temperatures below and above the critical point.

introduced in Ref. 4. We see that the second-order character is confirmed by the order parameters. We notice that for all the second-rank order parameters, the curves, obtained for the two system sizes, only differ at high temperatures, due to the isotropic statistical finite size limit for which the minimum value is of the order of $1/\sqrt{N}$. A more stringent test of the character of the transition is obtained by examining not only the average value of the order parameters, but a histogram of the values obtained from the simulation. Far from the transition, the histogram is expected to be a single-peaked Gaussian. However, near a transition we expect a different behavior for a first-order transition, which is expected to present two (ideally two equally populated) peaks corresponding to ordered and disordered states and a higher order transition which should always show a peak. In Fig. 7 we see that the histogram of $\langle U^* \rangle$, for a temperature above and below the transition that we estimate to be at $T^* = 1.09 \pm 0.03$, does not present any sign of the double peak observed e.g., for the LL model,¹¹ even if a skewness is observed. Indeed the histogram only supports the second-order character of the transition.

4. Conclusions

In conclusion we have shown that for the biaxial LL model the biaxial–uniaxial nematic transition only occurs within the useful temperature range of 10% of the clearing temperature for values of biaxiality of less than 3% from the dual value $\lambda_c = 1/\sqrt{6}$. Moreover we have provided computer simulation evidence that at λ_c the transition is a second-order one.

Acknowledgments

We thank MURST, University of Bologna and CNR for support. We are also grateful to Regione Emilia-Romagna CED for the use of their DEC AXP 7000-710.

References

1. M. J. Freiser, *Phys. Rev. Lett.* **24**, 1041 (1970).
2. J. P. Straley, *Phys. Rev. A* **10**, 1881 (1974).
3. (a) G. R. Luckhurst and S. Romano, *Mol. Phys.* **40**, 129 (1980); (b) R. Hashim, G. R. Luckhurst, and S. Romano, *Mol. Phys.* **53**, 1535 (1984); (c) R. Hashim, G. R. Luckhurst, F. Prata, and S. Romano, *Liq. Cryst.* **15**, 283 (1993).
4. F. Biscarini, C. Chiccoli, P. Pasini, F. Semeria, and C. Zannoni, *Phys. Rev. Lett.* **75**, 1803 (1995).
5. M. P. Allen, *Liq. Cryst.* **8**, 499 (1990).
6. S. M. Fan, I. D. Fletcher, B. Gundo, G. Kothe, G. R. Luckhurst, and K. Praefcke, *Chem. Phys. Lett.* **204**, 517 (1993).
7. A. Ferrarini, P. L. Nordio, E. Spolaore, and G. R. Luckhurst, *J. Chem. Soc. Faraday Trans.* **91**, 3177 (1995).
8. M. E. Rose, *Elementary Theory of Angular Momentum* (Wiley, New York, 1957).
9. P. A. Lebwohl and G. Lasher, *Phys. Rev. A* **6**, 426 (1972).
10. N. Metropolis, A. W. Rosenbluth, M. N. Rosenbluth, A. H. Teller, and E. Teller, *J. Chem. Phys.* **21**, 1087 (1953).
11. U. Fabbri and C. Zannoni, *Mol. Phys.* **58**, 763 (1986).
12. Z. Zhang, M. Zuckermann, and O. G. Mouritsen, *Mol. Phys.* **80**, 1195 (1993).